CFD-BASED OPTIMIZATION OF ACOUSTIC NOISE IN THE DIFFUSER SECTION OF AN EXPANSION VALVE

N.T. Basse[1] and J. Pawlik[1]

[1]Danfoss A/S, Refrigeration and Air Conditioning Controls, Nordborgvej 81, DK-6430, Denmark

nils.basse@danfoss.com

Abstract

Flow noise in electronic expansion valves is becoming important for customers. We perform transient, compressible computational fluid dynamics simulations to study acoustic flow noise generation for different diffuser geometries. The trend of the simulations agrees with earlier experimental findings.

1 Introduction

Electronic expansion valves (EEVs) [Tomczyk et al (2016)] are used as components in many applications, e.g. for variable refrigerant flow (VRF) systems. Since these systems are typically placed in buildings, there is a need for low-noise EEVs.

The overall field of study is acoustics [Kinsler et al (2000), Jacobsen et al (2011)] with a specific focus on flow-generated noise [Bose (2013)] and how that propagates through components to the inhabited area.

Flow noise downstream of expansion devices has previously been studied experimentally [Singh et al (1999)], where one finding was described as "surprising": A diffuser half-angle θ of 10 degrees generated less flow noise than a θ of 5 degrees. This is part of the motivation for our work: To understand the relationship between diffuser angle and flow noise. Gaining this knowledge would then enable us to optimize the diffuser angle. A related question is whether the diffuser angle influences flow noise generation, propagation, or both.

2 CFD simulations

We use computational fluid dynamics (CFD) [Versteeg and Malalasekera (2007)] simulations to study flow noise in simple geometries. The three geometries treated are shown in Figure 1 and meshes in the xy-plane are presented in Figure 2. Common features include:

- Flow from left to right
- A cone (left-hand side)
- A rounded orifice entrance (radius of curvature 1 mm, orifice diameter 2 mm)
- A choke [Nakayama (2018)] section (diameter 2 mm)
- Diameter after diffuser 4.5 mm

Each geometry has a different θ: 7 (geometry a), 15 (geometry b) and 25 (geometry c) degrees. The geometries are full 3D, with model sizes between 1.9 and 2.4 million elements.

We do pressure-based transient simulations; for turbulence, we use the scale-adaptive simulation (SAS) [Menter and Egorov (2010), Egorov et al (2010)] method with a production limiter.

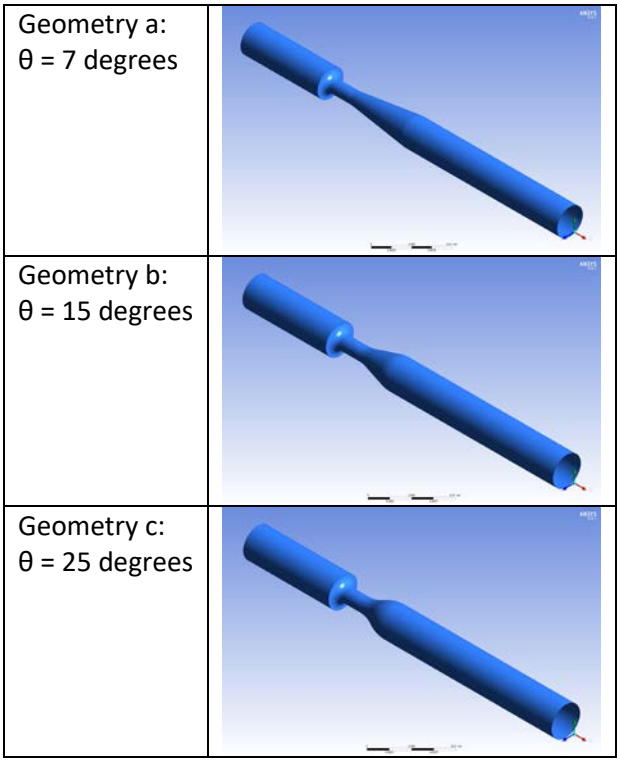

Figure 1: The three geometries simulated.

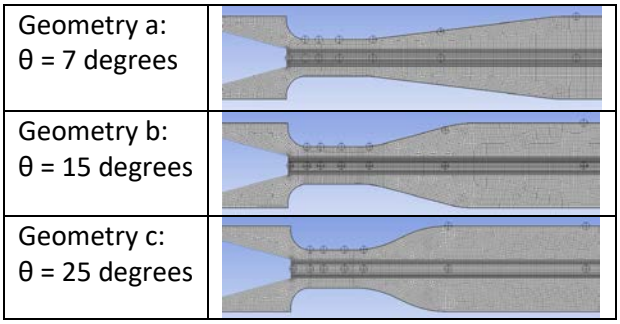

Figure 2: Meshes in the xy-plane of the three geometries simulated. Symbols (plusses inside circles) indicate static pressure monitor points.

A total of 265 000 timesteps are calculated after the simulation has reached stationary conditions. Each timestep is 1 μs, with a maximum of 20 iterations for each timestep. To reach convergence in few iterations, we reduced the continuity convergence criterion to 10^{-2}. Each simulation case takes several weeks to run using a 24-core workstation.

For expansion valves, typically the fluid at the valve inlet is single-phase; due to the large pressure loss through the valve orifice, the fluid at the outlet is two-phase. However, in some cases the inlet fluid might also consist of two phases. We model the refrigerant R410A as a single-phase compressible ideal gas with material properties which approximately match those observed in applications. The operating pressure is 0 Pa, the total inlet pressure is 20 bar and the gauge outlet pressure is 9.4 bar.

We operate under the overall assumption that there is a link between pressure loss and flow noise, i.e. measures to reduce the pressure loss will also reduce flow noise. A specific example is the diffuser angle. Traditionally, it is recommended to keep the diffuser angle below a certain value to avoid diffuser stall (detachment) which increases the pressure loss [Blevins (2003)]. However, as mentioned in [Singh et al (1999)], the opposite effect has been measured, i.e. that a larger diffuser angle results in lower flow noise.

3 Results

To verify the not-so-intuitive diffuser measurements in [Singh et al (1999)], we performed CFD simulations as outlined above.

The mass flow through the valve is shown in Figure 3 for the three geometries. The average values are almost identical, but important fluctuation differences can be seen:

- θ = 7 degrees: Continuous fluctuations
- θ = 15 degrees: Intermittent bursts of fluctuations interspersed with steady periods
- θ = 25 degrees: Steady

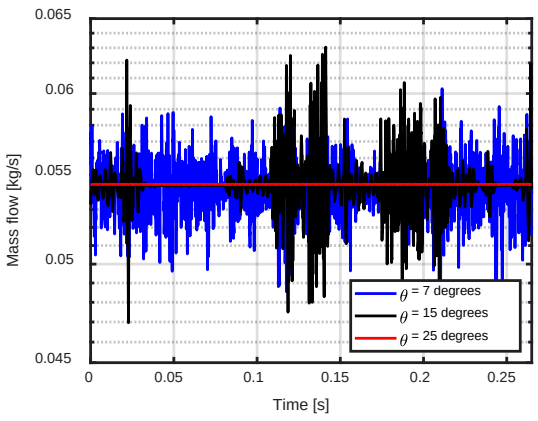

Figure 3: Mass flow versus time.

To monitor the static pressure, we placed on-axis and wall points as indicated by the symbols in Figure 2. The wall points are placed 2 μm from the wall.

To study the spectral components, we then calculated the power spectral density (PSD) over the entire time interval, see Figure 4. Two monitor points close to the wall are treated for each geometry, one close to the cone (point 8) and another one far from the cone (point 13).

Two differences stand out between the 7 and 15 degree diffusers compared to the 25 degree diffuser:

- The overall noise level is lower for 25 degrees compared to 7 and 15 degrees
- There are pronounced frequency peaks in the 25 degree spectra, most notably at 7 kHz and a harmonic peak at 14 kHz

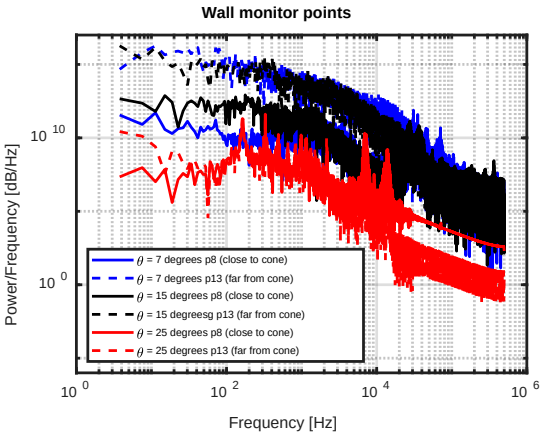

Figure 4: PSD of the static pressure at representative monitor points close to the wall.

As a next step to evaluate our results, we calculate the sound pressure level (SPL) for the one-third octave bands and perform an A-weighting, see Figure 5.

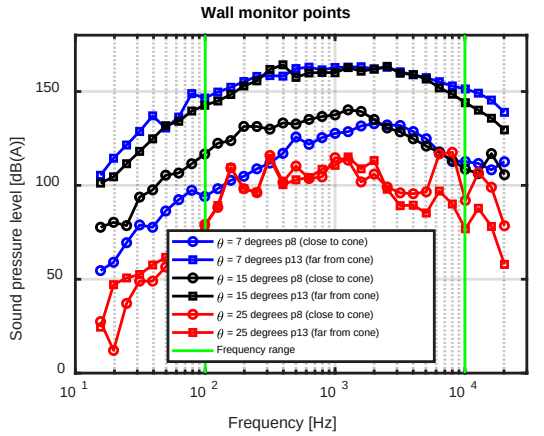

Figure 5: A-weighted one-third octave bands of the SPL at representative monitor points close to the wall. The vertical green lines indicate the frequency interval used for the sum of the sound pressure level.

From this analysis it is more clear that the overall noise level for 25 degrees is low compared to the other two geometries. For all geometries, the SPL spectrum is relatively flat.

Finally, we can create the sum of the A-weighted SPL (from 100 Hz to 10 kHz) for the three geometries and display it as a function of the distance from the cone tip, see Figure 6.

The noise level sum in the choke for 25 degrees is more than 10 dB(A) lower than for the two other geometries. In the diffuser section, this difference increases up to around 50 dB(A).

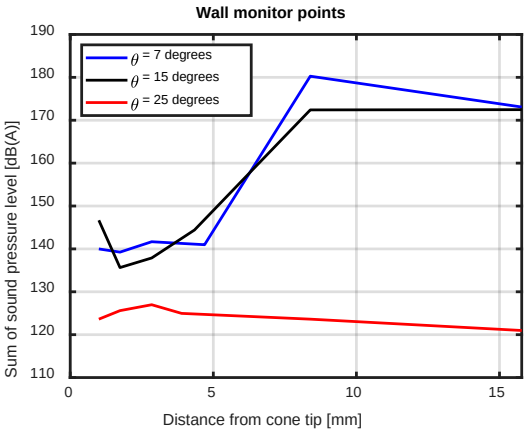

Figure 6: Sum of A-weighted one-third octave bands from 100 Hz to 10 kHz as a function of distance from the cone tip.

4 Discussion

For our discussion, we focus on simulations for the 7 and 25 degree diffusers.

We treat simulation results for the final time step. The 2D plots are for the xy-plane.

In Figure 7 we display the static pressure. Two steps of pressure loss can be observed, the first at the orifice and the second at the diffuser entrance (transition from the choke to the diffuser). Some pressure recovery is seen after the diffuser. There are no large asymmetries.

The velocity magnitude (speed) is shown in Figure 8. For 7 degrees, the jet from the choke is attaching to the upper part of the wall, whereas the jet for 25 degrees is symmetric through the diffuser. The highest velocity is at the diffuser entrance.

The total pressure can be found in Figure 9. The main decrease in total pressure is at the diffuser entrance. For both diffusers, the maximum total pressure after the choke is aligned with the choke. As for velocity, there is asymmetry for the total pressure of the 7 degree diffuser, but not for the 25 degree diffuser.

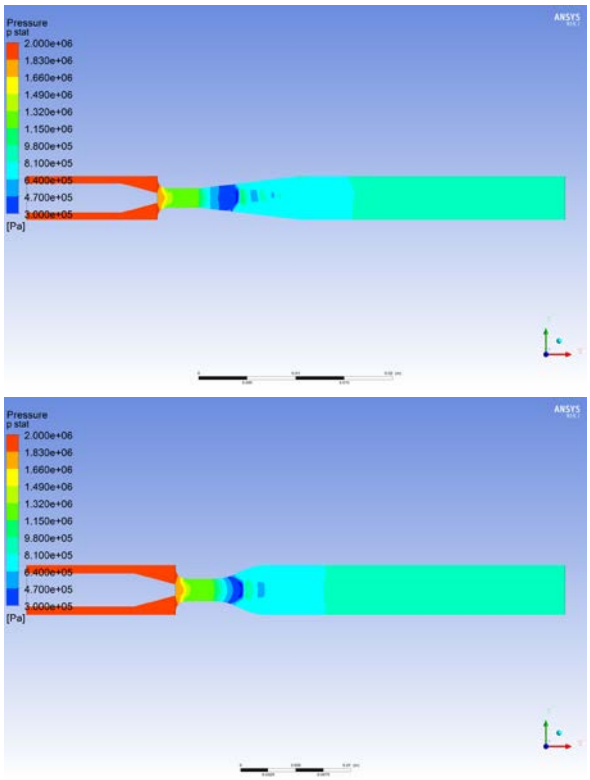

Figure 7: Static pressure in the xy-plane, top: θ = 7 degrees, bottom: θ = 25 degrees.

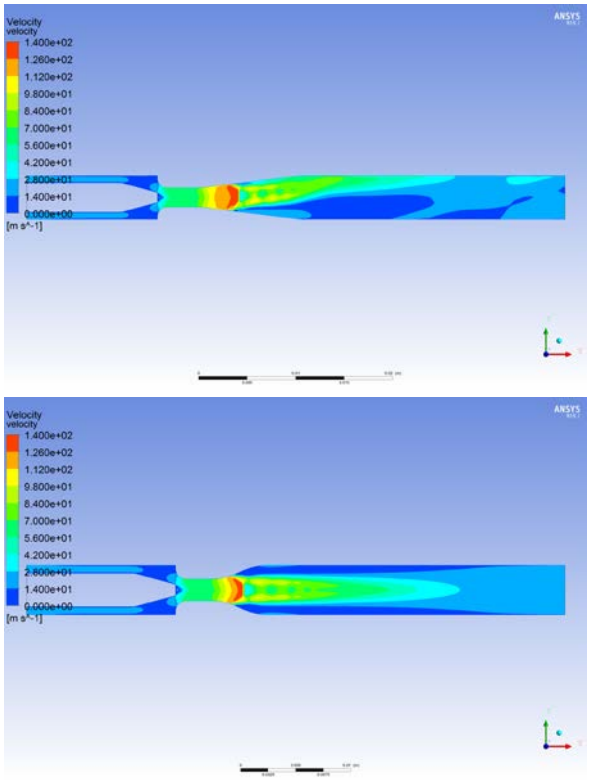

Figure 8: Velocity magnitude (speed) in the xy-plane, top: θ = 7 degrees, bottom: θ = 25 degrees.

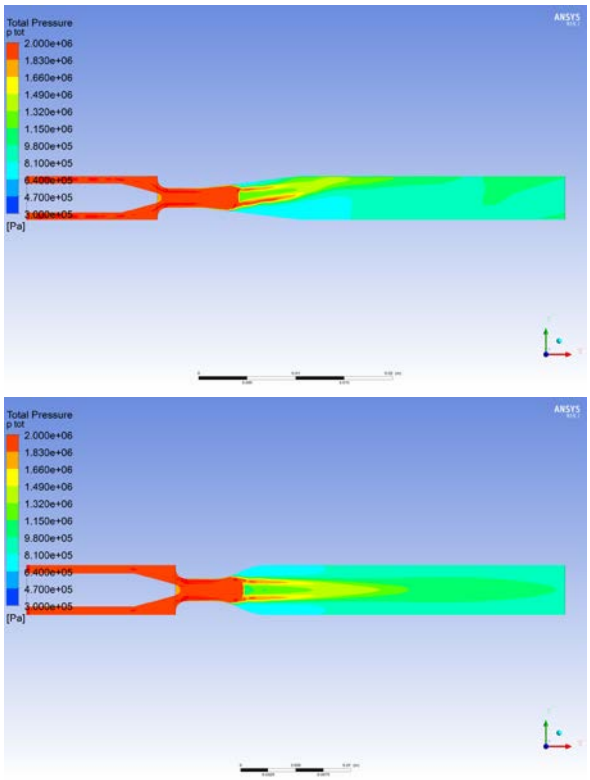

Figure 9: Total pressure in the xy-plane, top: θ = 7 degrees, bottom: θ = 25 degrees.

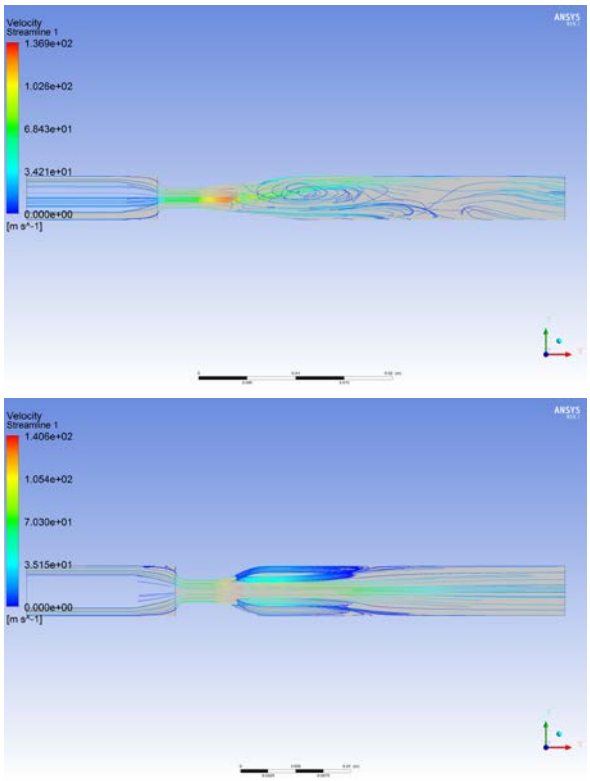

Figure 10: Velocity streamlines in the xy-plane, top: θ = 7 degrees, bottom: θ = 25 degrees.

Using 50 seed points from the xy-plane, streamlines are generated, see Figure 10. For 7 degrees, a vortex is seen at the top, while a symmetric vortex exists for 25 degrees. The vortex for 25 degrees has an approximate length of 5 mm and a speed of roughly 35 m/s. This yields an eddy-turnover time [Pope (2000)] of 143 µs, which can be regarded as an estimated lifetime of the vortex. That can be related to the 7 kHz peak for 25 degrees in Figure 4: This frequency corresponds to a period of 143 µs as well. We conclude that the 7 kHz signature is generated by the vortex in the diffuser.

For 25 degrees, the vortex in the diffuser is a vortex ring. This is visualized in Figure 11, where velocity streamlines are generated with 50 seed points from both the xy- and the xz-plane. The streamlines are viewed from the outlet. We observe that the streamlines for 7 degrees are covering the entire cross-section, whereas the streamlines for 25 degrees are confined to a torus.

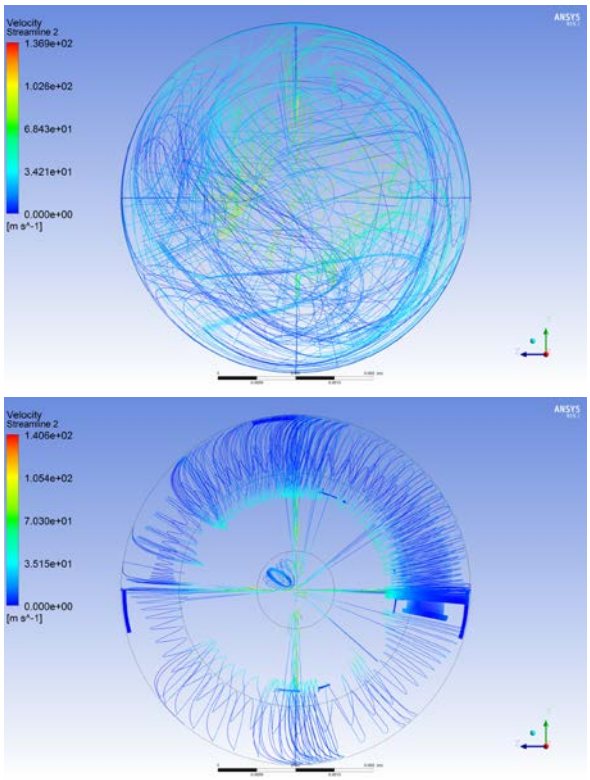

Figure 11: Velocity streamlines seen from the outlet, top: θ = 7 degrees, bottom: θ = 25 degrees.

The turbulence intensity (TI) [Russo and Basse (2016)] is shown in Figure 12. The maximum is of order 20% and located in the center of the vortices.

Our results indicate that differences in vortical structures are - at least partially – responsible for differences observed between the diffuser geometries. In Figure 13, we plot the vorticity [Saffman (1992)] magnitude on the wall. For both geometries, the vorticity is large in the choke. After the diffuser, a large local vorticity maximum is observed for the 7 degree diffuser (the maximum is dominated by vorticity in the z-direction). Such a maximum is not seen for the 25 degree diffuser. The small difference in the choke and larger difference after the diffuser

corresponds to the finding of the sum of the A-weighted SPL in Figure 6.

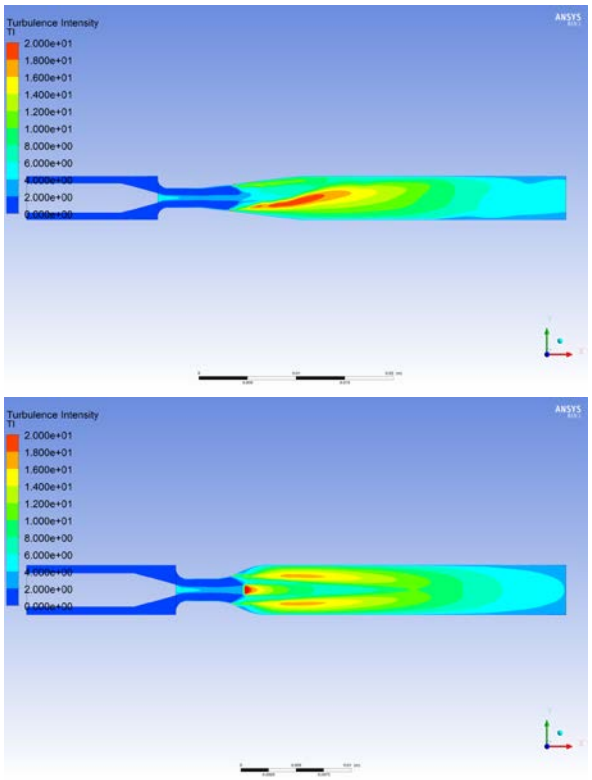

Figure 12: Turbulence intensity in the xy-plane, top: θ = 7 degrees, bottom: θ = 25 degrees.

The price which must be paid for an overall lower flow noise level appears to be the presence of a vortex ring in the diffuser: The vortex ring acts to isolate noise from reaching the wall.

If the discrete vortex frequency (and harmonics) is not exciting structural vibrations, this solution may be the best option.

Finally, we can investigate the helicity [Moffatt (1969), Moffatt and Tsinober (1992)], which is an indicator of the degree of "knottedness" of the vortex lines of the flow, see Figure 14. As for vorticity, we find that a large helicity magnitude is related to the case with more flow noise.

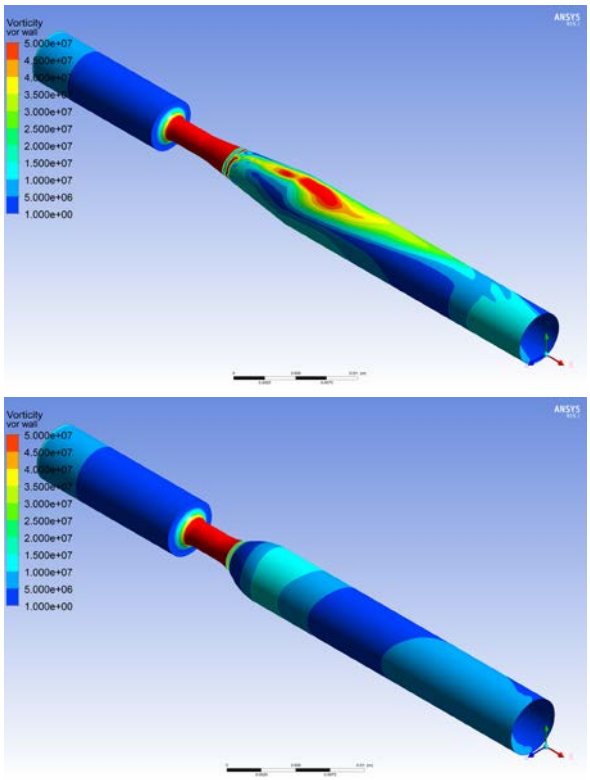

Figure 13: Vorticity at the wall, top: θ = 7 degrees, bottom: θ = 25 degrees.

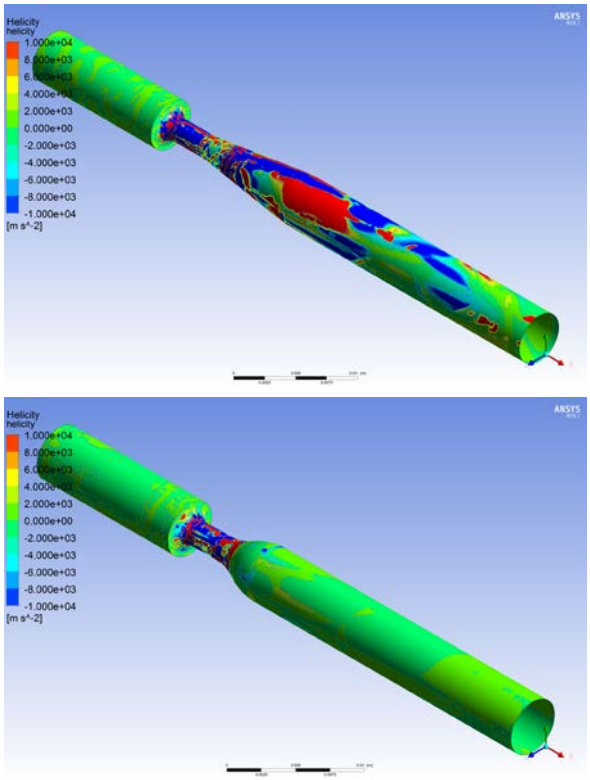

Figure 14: Helicity at the wall, top: θ = 7 degrees, bottom: θ = 25 degrees.

5 Conclusions

We have carried out CFD simulations to study the acoustic performance of different diffusers. The diffuser with largest angle displays the lowest noise level. The reason for this appears to be the existence of a vortex ring in the large-angle diffuser which acts to shield the wall from noise generated farther inside the flow. Thus, an abrupt expansion may also perform well. However, it has to be kept in mind that many valves are bidirectional.

Our simulations agree qualitatively with previous measurements. However, we note that the measurements were made more than 15 pipe diameters downstream of the valve. To make a one-to-one comparison, we should repeat our simulations with a long pipe downstream. This would also shed light on our question posed in the Introduction: Does the diffuser angle influence flow noise generation, propagation, or both?

Acknowledgements

We thank Love Håkansson at EDRMedeso for providing the initial CFD settings.

References

Blevins R.D. (2003), Applied Fluid Dynamics Handbook, Krieger Publishing Company.

Bose T. (2013), Aerodynamic Noise – An Introduction for Physicists and Engineers, Springer.

Egorov Y., Menter F.R., Lechner R. and Cokljat D. (2010), The Scale-Adaptive Simulation Method for Unsteady Turbulent Flow Predictions. Part 2: Application to Complex Flows, *Flow Turbulence Combust.* vol. 85, pages 139-165.

Jacobsen F., Poulsen T., Rindel J.H., Gade A.C. and Ohlrich M. (2011), Fundamentals of Acoustics and Noise Control, DTU Lecture Note 31200.

Kinsler L.E., Frey A.R., Coppens A.B. and Sanders J.V. (2000), Fundamentals of Acoustics, 4th Ed., John Wiley and Sons.

Menter F.R. and Egorov Y. (2010), The Scale-Adaptive Simulation Method for Unsteady Turbulent Flow Predictions. Part 1: Theory and Model Description, *Flow Turbulence Combust.* vol. 85, pages 113-138.

Moffatt H.K. (1969), The Degree of Knottedness of Tangled Vortex Lines, *J. Fluid Mech.* vol. 35, pages 117-129.

Moffatt H.K. and Tsinober A. (1992), Helicity in Laminar and Turbulent Flow, *Annu. Rev. Fluid Mech.* vol. 24, pages 281-312.

Nakayama Y. (2018), Introduction to Fluid Mechanics, 2nd Ed., Butterworth-Heinemann.

Pope S.B. (2000), Turbulent Flows, Cambridge University Press.

Russo F. and Basse N.T. (2016), Scaling of Turbulence Intensity for Low-Speed Flow in Smooth Pipes, *Flow Meas. Instrum.* vol. 52, pages 101-114.

Saffman P.G. (1992), Vortex Dynamics, Cambridge University Press.

Singh G.M., Rodarte E., Miller N.R. and Hrnjak P.S. (1999), Noise Generation from Expansion Devices in Refrigerant, ACRC Report TR-152.

Tomczyk J., Silberstein E., Whitman B. and Johnson B. (2002), Refrigeration and Air Conditioning Technology, 8th Ed., Cengage Learning.

Versteeg H.K and Malalasekera W. (2007), An Introduction to Computational Fluid Dynamics – The Finite Volume Method, 2nd Ed., Pearson Education Limited.